Investigation of Pitting Corrosion Rate on Micro Plasma Arc Welded Dissimilar Weld Joints of AISI 304 and AISI 430 Stainless Steel Sheets

G. Uma Maheswara Rao[1, *]
Department of Mechanical Engineering,
Anil Neerukonda Institute of Technology & Sciences, India
E-mail: gumr.anits@gmail.com
*Corresponding author

Ch. Srinivasa Rao [2]
Department of Mechanical Engineering,
Andhra University, India
E-mail: csr_auce@yahoo.co.in

Received: 28 April 2020, Revised: 27 May 2020, Accepted: 22 July 2020

Abstract: In the present paper investigation is carried out to study pitting corrosion rate of Pulsed Current Micro Plasma Arc welded AISI304 and AISI430 dissimilar joint in three different mediums namely 0.5N NaOH, 3.5N NaCl and 0.5N HCl. Linear Polarization method is used and Tafel are drawn, from which corrosion rates are evaluated in Heat Affected Zone (HAZ) of AISI 304, AISI 430 and at Fusion zone (FZ) of the weld joint. Corrosion pits are studied using Scanning Electron Microscope (SEM) images. It is revealed that AISI 304 is subjected to more corrosion when compared to AISI 430. Corrosion rate is higher in HCl when compared to NaCl and NaOH mediums. Corrosion rate is high at FZ, than HAZ of AISI 304 and AISI 430.

Keywords: AISI 430, AISI 304, Micro Plasma Arc Welding, pitting corrosion

Reference: G. Uma Maheswara Rao, and Ch. Srinivasa Rao, "Investigation of pitting corrosion rate on Micro Plasma arc welded dissimilar weld joints of AISI 304 and AISI 430 stainless steel sheets", Int J of Advanced Design and Manufacturing Technology, Vol. 13/No. 3, 2020, pp. 59–66.
DOI: 10.30495/admt.2020.1898623.1195

Biographical notes: G. Uma Maheswaea Rao is Senior Assistant Professor of Mechanical Engineering at Anil Neerukonda Institute of Technology and Sciences, India. His research interest includes manufacturing and optimization**. Ch. Srinivasa Rao** is Professor of Mechanical engineering at the Andhra University, India. He received his PhD in Mechanical engineering from Andhra University of India. He has guided 12 PhD students and published 80 papers in International Journals. His current research focuses on Welding and Metal forming.

1 INTRODUCTION

Dissimilar metal welds between austenitic and ferritic stainless steels with low carbon content are extensively utilized in many high temperature applications such as energy conversion systems. For instance, in central power stations, sections of the boilers subjected to lower temperature are made from ferritic stainless steel for economic reasons. The other operating at higher temperatures, are constructed with austenitic stainless steel. Therefore, the transition welds are needed between the two stainless steels [1-2]. A wide range of industries including chemicals, pharmaceuticals, textiles, food, drink, pulp and paper are using ferritic-austenitic stainless steel.

Joining of dissimilar metals is really a challenging task due to difference in their thermal, mechanical and chemical properties welded under a common welding condition. A variety of problems evolves in dissimilar welding like cracking, large weld residual stress, migration of atoms during welding causing stress concentration on one side of the weld, compressive and tensile stresses, stress corrosion cracking etc. To overcome these challenges, it is required to study the effect of welding process parameter on mechanical property. However, joining of dissimilar metals has found its use extensively in power generation, electronic, petrochemical and chemical industries, nuclear reactors due to environmental concerns, energy saving, high performance, cost saving and so on.

From the literature review it is understood that Ramesh Kumar S et al. [3] carried out PAW on AISI 304 austenitic and AISI 430 ferritic stainless steel combination in this paper.They studied parameter optimization, microstructural behavior and mechanical properties. G. Madhusudan Reddy et al. [4] studied Microstructure and mechanical properties of similar and dissimilar welds of austenitic stainless steel (AISI 304), ferritic stainless steel (AISI 430) and duplex stainless steel (AISI 2205) joined using electron beam welding and friction welding.

Lokesh Kumar et al. [5] investigated the effect of current on the microstructure and mechanical properties in SMAW and GTAW process, formed by AISI 304 (ASS) and AISI 430 (FSS) with AWS E308L austenitic stainless steel covered electrode. M.M.A. Khan et al. [6] carried out laser beam welding of dissimilar AISI 304L and AISI 430 stainless steels. Experimental studies were focused on effects of laser power, welding speed, defocus distance, beam incident angle, and line energy on weld bead geometry and shearing force. Saeid Ghorbania et al. [7] joined dissimilar austenitic stainless steel (AISI 304L) and ferritic stainless steel (AISI 430) have been welded with two types of filler metals (316L and 2594L) by GTAW and studied the effect of heat treatment on the microstructure, mechanical properties, and corrosion properties of welded joint. R. Ghasemi et al. [8] performed GTAW welding of AISI 304 to AISI 430 stainless steel. Three filler metals including ER309L, ER316L and ER2594 were applied.

A. Arun Mani et al. [9] studied microstructural characteristic of dissimilar welded components (AISI 430 ferritic-AISI 304 austenitic stainless steels) by CO2 laser beam welding (LBW). Sarah S Farhood et al. [10] investigated the effect of pulsed Nd-YAG laser welding of AISI 304 to AISI 430 stainless steel was investigated. Laser parameters such as (peak power, pulse duration and welding speed) were changed and the change in properties was measured. G. Madhusudhan Reddy et al. [11] studied dissimilar metal welding of austenitic (AISI 304)-ferritic (AISI 430) stainless steel has been taken up to understand the influence of the welding process on microstructure and mechanical properties.

From the earlier works it is understood that most of the corrosion studies are carried out in chloride medium, but no works are reported on Plasma arc welded samples. In the present work Pulsed Current Micro Plasma Arc Welding (MPAW) is used to join two dissimilar AISI 304 and AISI 430 sheets of 0.4mm thick. Pitting corrosion tests are carried out using Linear polarization method and corrosion rates at three different medium namely NaOH, NaCl and HCl are computed.

2 EXPERIMENTATION

2.1. Plasma Arc Welding

Two dissimilar steels of AISI 304 and AISI 430 of 0.4mm thick sheets of 100 x 150 x 0.4 mm are welded autogenously with square butt joint without edge preparation. The chemical composition of two dissimilar AISI 304 and AISI 430 sheets of 0.4mm thick sheet is given in “Table 1 and 2”.

Table 1 Chemical composition of AISI 304 (weight %)

C	Si	Mn	P	S	Cr	Mo	Ni	Al
0.063	0.437	0.939	0.030	0.002	18.630	0.250	8.090	0.001
Co	Cu	Nb	Ti	V	W	Pb	Fe	N
0.215	0.366	0.028	0.008	0.166	0.053	-	70.600	-

Table 2 Chemical composition of AISI 430 (weight %)

C	Si	Mn	P	S	Cr	Mo	Ni	Al
0.055	0.383	0.343	0.007	0.002	16.860	0.073	0.130	0.002
Co	Cu	Nb	Ti	V	W	Pb	Fe	N
0.006	0.038	0.032	0.003	0.135	0.025	-	81.700	-

High purity argon gas (99.99%) is used as a shielding gas and a trailing gas right after welding to prevent absorption of oxygen and nitrogen from the atmosphere. The welding has been carried out under the welding conditions presented in "Table 3".

Table 3 Welding conditions

Power source	**Secheron Micro Plasma Arc Machine (Model: PLASMAFIX 50E)**
Polarity	DCEN
Mode of operation	Pulse mode
Electrode	2% thoriated tungsten electrode
Electrode Diameter	1.5 mm
Plasma gas	Argon & Hydrogen
Plasma gas flow rate	6 Lpm
Shielding gas	Argon
Shielding gas flow rate	6 Lpm
Purging gas	Argon
Purging gas flow rate	4 Lpm
Copper Nozzle diameter	1mm
Nozzle to plate distance	1mm
Welding speed	230 mm/min
Torch Position	Vertical
Operation type	Automatic
Peak current	20 Amperes
Base current	16 Amperes
Pulse rate	30 pulses/second
Pulse width	40 %

The values of process parameters used in this study are the optimal values obtained from our earlier papers [12-13]. Details about experimental setup are shown in "Fig. 1".

Fig. 1 Micro Plasma Arc Welding Setup.

2.2. Measurement of Pitting Corrosion Rate

AISI 304 and 430 steels has good resistance to corrosion, however when it is subjected to severe heating during welding processes, there is a possibility of corrosion effect on the welded joint. Welded joints of AISI 304 and 430 steels are subjected to pitting corrosion when exposed to different environments. The pitting corrosion rate depends upon the type, concentration of the exposed environment and exposure time of the welded joint. The details about sample preparation and testing procedure for measurement of pitting corrosion rate are discussed in the following sections.

2.2.1. Surface Preparation for Plating

The welded test specimen surface is polished with 220 and 600 mesh size emery papers in the presence of distilled water continuously. The polished specimen is first rinsed with distilled water, cleaned with acetone and again rinsed with distilled water to remove the stains and grease. Finally, the specimen is dried to remove the moisture content on the surface of the sample.

2.2.2. Sample Preparation for Corrosion studies

Once the sample is cleaned as per the procedure mentioned in section 2.1, the entire sample is covered by nail polish and only a cross sectional area of 10 cm^2 is exposed The electrochemical cell (test specimen with tube) ("Fig. 2").

Fig. 2 Electrochemical cell.

2.2.3. Procedure for Corrosion Studies

Around 200 ml of filtered electrolyte is poured into the electrochemical cell. The entire electrode assembly is now placed in the cell. The reference electrode (standard calomel electrode) is adjusted in such a way that the tip of this electrode is very near to the exposed area of working electrode (test specimen). The auxiliary platinum electrode is also placed in the cell. Now the cell assembly has been connected to the AUTOLAB/PGSTAT12. The black colored plug has been connected to the auxiliary electrode, red colored plug to the working electrode and blue to the reference electrode. The sample has been exposed to electrolytic medium for a span of 30 minutes.

As the start button of the potentiostat is switched on, the electrode potential changes continuously, till the reaction between the electrode and the medium attains equilibrium. After some time, the potential remains nearly constant without any change. This steady potential which is displayed on the monitor is taken as open circuit potential (E_{rest}). Now the equipment is ready for obtaining the polarization data.

Potential is scanned cathodically until the potential is equal to E_{rest} minus the limit potential. Measurements of potential (E) and current (I) are made at different intervals and the data is displayed on the monitor itself as E vs log I plot. After reaching the cathodic limit, the scan direction is then reversed. Similarly, anodic polarization data is obtained. The scan is again reversed and finally terminated and the cell is isolated from the potentiostat when the potential reached E_{rest}. The data recorded gives the Tafel plot (current vs potential data). Using the software available corrosion rate, corrosion current, polarization resistance and Tafel slopes are evaluated by Tafel plot and curve fit Tafel plot methods.

2.2.4. Corrosion Testing Methodology

Aggressive ions of chloride solutions are susceptible to pitting corrosion. This type of corrosion is potential-dependent and its occurrence is observed only above the pitting potential (E_{corr}), which can be used to differentiate the resistance to pitting corrosion of different metal/electrolyte systems. The E_{corr} value can be determined electrochemically using both potentiostatic and potentiodynamic techniques.

2.2.5. Linear Polarization method

The linear polarization method utilizes the Tafel extrapolation technique. The electrochemical technique of polarization resistance is used to measure absolute corrosion rate, usually expressed in milli-inches per year (mpy), which is further converted in to mm per year. Polarization resistance can be recorded in few minutes and correlation can often be made between corrosion rates obtained by polarization resistance and conventional weight-change determinations. Polarization resistance is also referred to as "linear polarization". Polarization resistance measurement is performed by scanning through a potential range which is very close to the corrosion potential, E_{corr} the potential range is generally ±25 mV about E_{corr}. The resulting current vs. potential is plotted, as shown in "Fig. 3".

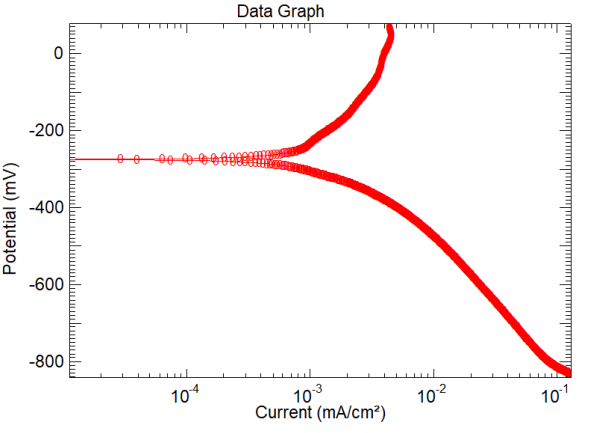

Fig. 3 Tafel Plot.

The corrosion current, I_{corr} is related to the slope of the plot through the following equation:

$$\frac{\Delta E}{\Delta I} = \frac{\beta_a \beta_c}{2.3 I_{corr}(\beta_a + \beta_c)} \quad \ldots \quad \ldots..(1)$$

Where $\Delta E/\Delta I$ = slope of the polarization resistance plot, where ΔE is expressed in volts and ΔI in µA. This slope has units of resistance, hence, polarization Resistance. β_a, β_c are anode and cathode Tafel constants (must be determined from a Tafel plot).

These constants have the units of volts/decade of current.

I_{corr} = corrosion current, µA.

Rearranging equation (5.1)

$$I_{corr} = \frac{\beta_a \beta_c}{2.3(\beta_a + \beta_c)} \frac{\Delta I}{\Delta E} \quad \ldots \quad \ldots(2)$$

The corrosion current can be related to the corrosion rate through the following equation.

Corrosion rate (mpy) = $0.131(I_{corr})(Eq.Wt)/\rho$ ….(3)

Where:

Eq.Wt = equivalent weight of the corroding species

ρ = density of the corroding species, g/cm^3

I_{corr} = corrosion current density, $\mu A/cm^2$

2.2.6. Tafel Analysis

The polarization data on E and I are plotted on a semi-logarithmic plot with current on x-axis (logarithmic

scale) as shown in "Fig. 3". From the Tafel plot [9-10] polarization data could be graphically obtained and theoretically evaluated. The slopes of the anodic and cathodic polarization curves, β_a and β_c both in anodic and cathodic regions are obtained from "Fig. 4". Using this data, corrosion current density I_{corr} is calculated from the equation (4) as shown below [10-11]:

$$I_{corr} = \frac{1}{2.3}\frac{\beta_a\beta_c}{(\beta_a+\beta_c)}\frac{1}{R_P} \quad \ldots(4)$$

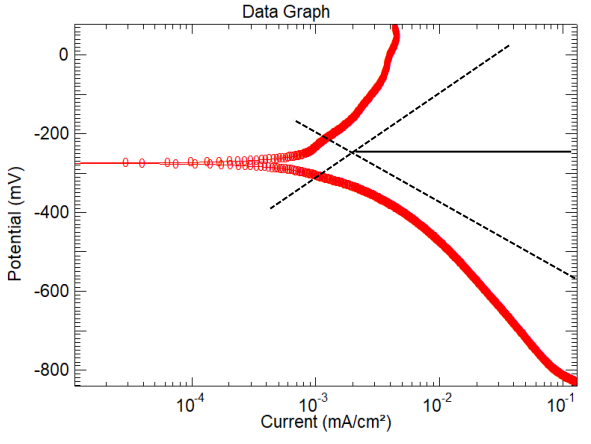

Fig. 4 Tafel Analysis.

$$R_P^{-1} = \frac{1}{R_P} = \left(\frac{\Delta I}{\Delta E}\right)E_{rest} \quad \ldots.(5)$$

Where:

R_p is polarization resistance
β_a and β_c are anodic and cathodic Tafel slopes
I_{corr} and E_{rest} are corrosion current density and rest potential.
Corrosion Rates are calculated from the equations (6) to (8).

$$\text{Corrosion rate } (CR_{mpy}) = 0.131(I_{corr})(Eq.Wt)/\rho \quad . \quad . (6)$$

$$\text{Corrosion rate } (CR_{mdd}) = \frac{CR_{mpy}\rho}{1.44} \quad \ldots \quad (7)$$

$$\text{Corrosion rate } (CR_{mm/yr}) = CR_{mpy} \times 2.52 \times 10^{-2} \quad (8)$$

The time duration for explosion of the corrosion medium is about 30 minutes and linearly polarized both anodically and cathodically within a close range of potentials E_{rest} ± 30mV. Scan rate (Scan rate = 1 mV/s) were maintained as per the ASTM G59-97 standard. The data recorded for each set are analysed using Tafel method.
The limitation of "Tafel method" is that β_a and β_c values are estimated to an approximation by drawing tangents in the linearly polarized regions of anodic and cathodic polarization curves. Hyperbolic nature of the polarized curve is taken as the best approximation. Tafel plots for 0.5N NaOH, 3.5N NaCl and 0.5N HCl are shown in "Fig. 5".

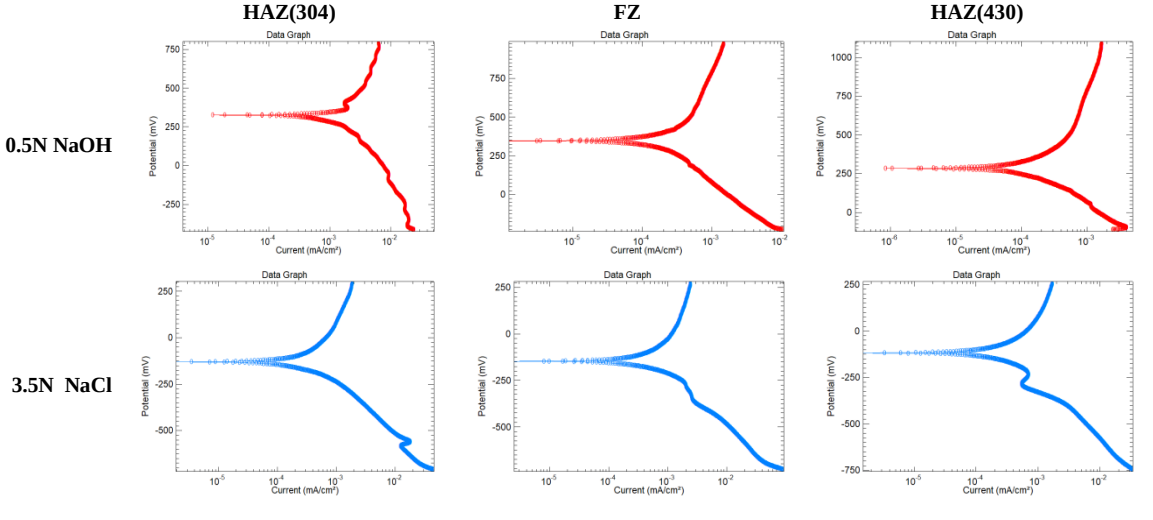

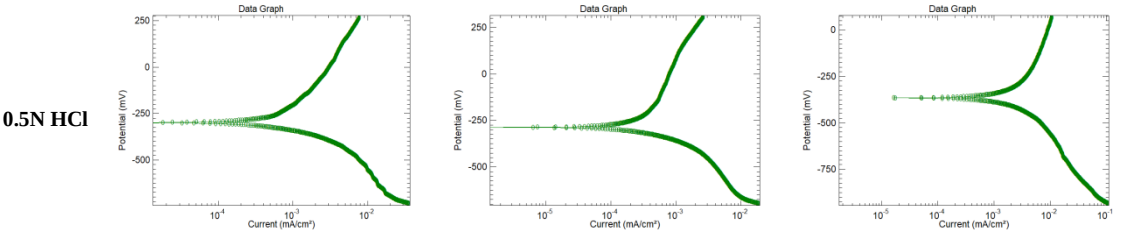

Fig. 5 Tafel plots for different weld samples.

Figure 6 indicates the SEM images at HAZ(304), Fusion Zone (FZ), HAZ(430) areas of weld joint exposed to 0.5N NaOH, 3.5N NaCl and 0.5N HCl medium. Corrosion pits (white spots) are clearly seen, which indicates attack of pitting corrosion. In 0.5N NaOH the corrosion rate is very low, when compared to 3.5N NaCl and 0.5 N HCl in all the three zones. The measured values are presented in "Table 4". ("Fig. 7")

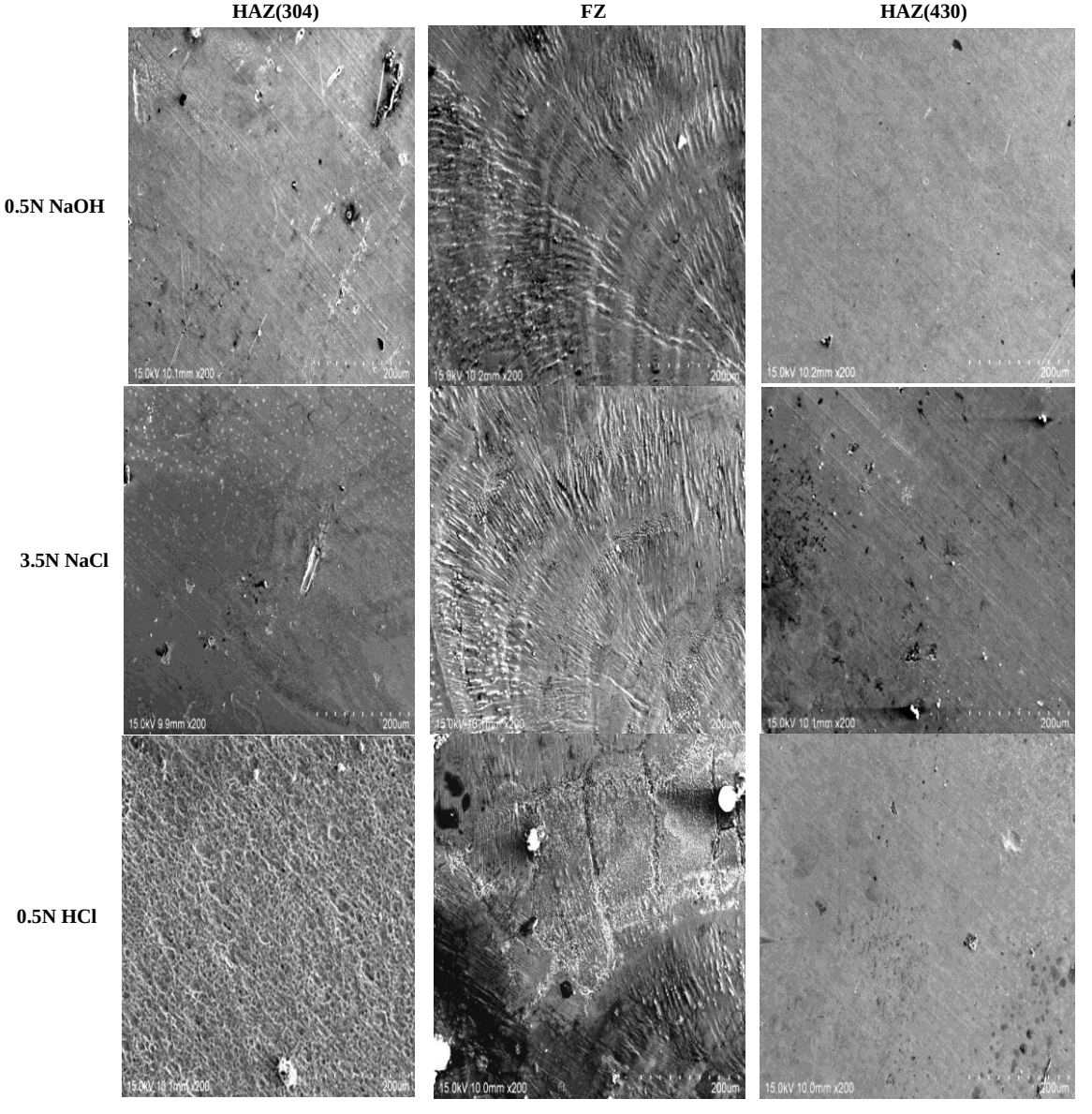

Fig. 6 SEM images of weld samples.

Table 4 Experimental values

	Corrosion potential (E_{corr}, mV)	Corrosion current density (I_{corr}, mA/cm^2)	Anodic Tafel slope (β_a, mV)	Cathodic Tafel slope (β_c, mV)	Corrosion rate (mm/year)	Corrosion rate (mils/year)
Sample name	Parameter (0.5N NaOH)					
304(HAZ)	325.32	0.0024605	458.48	441.98	0.0214590	0.8448419
FZ	454.51	0.0017388	1083.6	439.92	0.0151273	0.5955628
430(HAZ)	152.16	0.0006566	868.98	274.47	0.0057125	0.2249004
Sample name	Parameter (3.5N NaCl)					
304(HAZ)	-187.84	0.0025514	1066.6	404.60	0.0221975	0.8739176
FZ	-205.86	0.0065095	952.18	369.31	0.0566324	2.2296000
430(HAZ)	-133.58	0.0019320	788.24	413.0	0.0168085	0.6617513
Sample name	Parameter (0.5N HCl)					
304(HAZ)	-286.02	0.0071227	783.47	247.02	0.0619672	2.4396
FZ	-543.69	0.0102353	331.93	207.28	0.0890472	3.5057
430(HAZ)	-310.01	0.0034504	596.09	156.10	0.0300185	1.1818

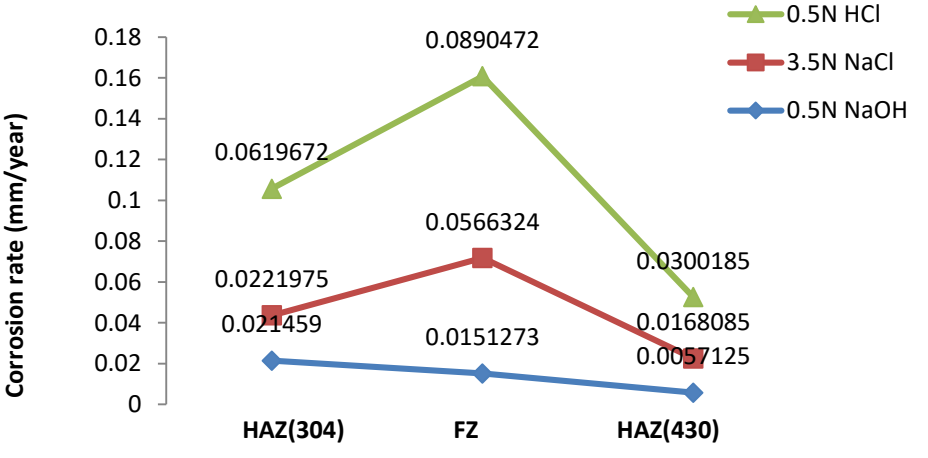

Fig. 7 Variation of corrosion rate.

3 CONCLUSIONS

The following conclusions are drawn based on the experiments performed:

1) Pitting corrosion test was performed on dissimilar welded joints of AISI 304 and AISI 430 using Linear Polarization method.
2) From the corrosion rate values, it is understood that the weld joints are more passive in 0.5N NaOH medium in Heat Affected Zone of AISI 304, Heat Affected Zone of 430 and Fusion Zone.
3) AISI 304 and AISI 430 are slightly subjected to pitting corrosion in chloride medium.
4) Fusion Zone is subjected to more corrosion rate when compared to Heat Affected Zone, this is because of fusion zone subjected to more heat during welding and also there are chances of depletion of some elements like chromium during welding.
5) The order of corrosion severity is HCl, NaCl and NaOH.

4 SCOPE OF WORK

The work is carried out at room temperature and at fixed normalities. One may perform corrosion test at elevated temperature and different normalities.

5 ACKNOWLEDGMENTS

We would like to thank Dr. Archana Mallik, Dept. of Metallurgy & Materials Engineering, NIT Rourkela for providing the corrosion facility.

REFERENCES

[1] Missori, S., Koerber, C., Laser Beam Welding of Austenitic Ferritic Transition Joints Weld. J. Vol. 76, 1997, pp. 125.

[2] Sireesha, M., Shankar, V., Albert S. K., and Sundaresan, S., Influence of High-Temperature Exposure On the Microstructure and Mechanical Properties of Dissimilar Metal Welds Between Modified 9Cr-1Mo Steel and Alloy 800 Mater. Sci. Eng., Vol. 292A, 2000, pp. 74–82.

[3] Ramesh Kumar, S., Singh, A. K., and Sandeep, S., Aravind P., Investigation on Microstructural Behavior and Mechanical Properties of Plasma Arc Welded Dissimilar Butt Joint of Austenitic- Ferritic Stainless Steels, Materials Today: Proceedings, Vol. 5, 2018, pp. 8008–8015.

[4] Madhusudan Reddy, G., Srinivasa Rao, K., Microstructure and Mechanical Properties of Similar and Dissimilar Stainless Steel Electron Beam and Friction Welds, Vol. 45, 2009, pp. 875-888.

[5] Lokesh Kumar, G., Karthikeyan, P., Narasimma Raj, C., and Prasanna, B., George Oliver, Microstructure And Mechanical Properties Of ASS (304)-FSS (430) Dissimilar Joints In SMAW & GTAW Process, 2015, pp. 367-378.

[6] Khana, M. M. A., Romoli, L., FiaschiA. M., Dini, B. G., and Sarri, A. F., Laser Beam Welding of Dissimilar Stainless Steels in a Fillet Joint Configuration, Journal of Materials Processing Technology, Vol. 212, 2012, pp. 856–867.

[7] Ghorbania, S., Ghasemib, R., Ebrahimi-Kahrizsangia, R., and Hojjati-Najafabadid, A., Effect of Post Weld Heat Treatment (pwht) on the Microstructure, Mechanical Properties, and Corrosion Resistance of Dissimilar Stainless Steels, Materials Science & Engineering A, Vol. 688, 2017, pp. 470–479.

[8] Ghasemi, R., Beidokhti, B., and Fazel-Najafabadi, M., Effect of Delta Ferrite on The Mechanical Properties of Dissimilar Ferritic-Austenitic Stainless Steel Welds, Arch. Metall. Mater., Vol. 63, 2018, pp. 437-443.

[9] Arun Mani, A., Senthil Kumar, T., and Chandrasekar, M., Mechanical and Metallurgical Properties of Dissimilar Welded Components (AISI 430 Ferritic – AISI 304 Austenitic Stainless Steels) by CO2 Laser Beam Welding (LBW), Journal of Chemical and Pharmaceutical Sciences, Special Vol. 6, 2015, pp.35-338.

[10] Farhood, S., Almurshdy, J. M., and Roubaiy, A. O. A., Welding of AISI 304 To AISI 430 Stainless Steel by Pulsed Nd-YAG Laser, Journal of Scientific and Engineering Research, Vol. 3, No. 1, 2016, pp. 44-50.

[11] Madhusudhan Reddy, G., Mohandas, T., Sambasiva Rao, A., and Satyanarayana, V. V., Influence of Welding Processes On Microstructure and Mechanical Properties of Dissimilar Austenitic-Ferritic Stainless Steel Welds, Vol. 20, No. 2, 2005, pp. 147-173.

[12] Uma Maheswara Rao, G., Srinivasa Rao, CH., Optimizing Fusion Zone Grain Size, Hardness and Tensile Strength of Pulsed Current Micro Plasma Arc Welded AISI 304 and AISI 430 dissimilar Alloy using Grey Relational Analysis, Journal of Mechanical and Mechanics Engineering, Vol. 5, No. 1, 2019, pp. 38-50.

[13] Siva Prasad, K., Srinivasa Rao, CH., and Nageswara Rao, D., Optimizing Fusion Zone Grain Size and Ultimate Tensile Strength of Pulsed Current Micro Plasma Arc Welded Inconel 625 Alloy Sheets using Hooke & Jeeves Method, International Transaction Journal of Engineering, Management & Applied Sciences & Technologies, Vol. 3, No. 1, 2012, pp. 87-100.